Title	Carboxylic acids production and electrosynthetic microbial community evolution under different CO2 feeding regimes
Author(s)	Dessì, Paolo; Sánchez, Carlos; Mills, Simon; Cocco, Francesco Giuseppe; Isipato, Marco; Ijaz, Umer Z.; Collins, Gavin; Lens, Piet N.L.
Publication Date	2020-10-15
Publication Information	Dessì, Paolo, Sánchez, Carlos, Mills, Simon, Cocco, Francesco Giuseppe, Isipato, Marco, Ijaz, Umer Z., Collins, Gavin, Lens, Piet N. L. (2021). Carboxylic acids production and electrosynthetic microbial community evolution under different CO2 feeding regimens. Bioelectrochemistry, 137, 107686. doi:https://doi.org/10.1016/j.bioelechem.2020.107686
Publisher	Elsevier
Link to publisher's version	https://doi.org/10.1016/j.bioelechem.2020.107686
Item record	http://hdl.handle.net/10379/16456
DOI	http://dx.doi.org/10.1016/j.bioelechem.2020.107686

Carboxylic acids production and electrosynthetic microbial community evolution under different CO_2 feeding regimens

Paolo Dessì [a,*], *Carlos Sánchez* [a], *Simon Mills* [a], *Francesco Giuseppe Cocco* [a,b], *Marco Isipato* [a,b], *Umer Z. Ijaz* [c], *Gavin Collins* [a], *Piet N. L. Lens* [a]

[a] *Microbiology, School of Natural Sciences and Ryan Institute, National University of Ireland Galway, University Road, Galway, H91 TK33, Ireland*

[b] *Department of Civil and Environmental Engineering and Architecture, University of Cagliari, Piazza d'Armi, 09123 Cagliari, Italy*

[c] *Infrastructure and Environment Research Division, School of Engineering, University of Glasgow, Oakfield Avenue, Glasgow G12 8LT, United Kingdom*

Manuscript submitted to: Bioelectrochemistry

*****Corresponding author: Phone: +353 830678774, e-mail: paolo.dessi@nuigalway.ie, mail: National University of Ireland Galway, Microbiology, School of Natural Sciences and Ryan Institute, University Road, Galway, H91 TK33, Ireland

Abstract

Microbial electrosynthesis (MES) is a potential technology for CO_2 recycling, but insufficient information is available on the microbial interactions underpinning electrochemically-assisted reactions. In this study, an MES reactor was operated for 225 days alternately with bicarbonate or CO_2 as carbon source, under batch or continuous feeding regimens, to evaluate the response of the microbial communities, and their productivity, to dynamic operating conditions. A stable acetic acid production rate of 9.68 g/m^2/d, and coulombic efficiency up to 40%, was achieved with continuous CO_2 sparging, higher than the rates obtained with bicarbonate (0.94 g/m^2/d) and CO_2 under fed-batch conditions (2.54 g/m^2/d). However, the highest butyric acid production rate (0.39 g/m^2/d) was achieved with intermittent CO_2 sparging. The microbial community analyses focused on differential amplicon sequence variants (ASVs), allowing detection of ASVs significantly different across consecutive samples. This analysis, combined with co-occurence network, and cyclic voltammetry, indicated that hydrogen-mediated acetogenesis was carried out by *Clostridium*, *Eubacterium* and *Acetobacterium*, whereas *Oscillibacter* and *Caproiciproducens* were involved in butyric acid production. The cathodic community was spatially inhomogeneous, with potential electrotrophs, such as *Sulfurospirillum* and *Desulfovibrio*, most prevalent near the current collector. The abundance of *Sulfurospirillum* positively correlated with *Acetobacterium*, supporting the syntrophic metabolism of both organisms.

Keywords: Bioelectrochemistry; Chain elongation; CO_2 electroreduction; Cyclic voltammetry; Microbial electrosynthesis; Miseq Sequencing.

1. Introduction

Increasing atmospheric CO_2 concentrations poses a challenge for sustainable economic development at global level. Legislative action by the European Union, for example, resulted in a 22% reduction of greenhouse gas emissions between 1990 and 2017, but additional measures are required to achieve a climate-neutral economy by 2050 [1], and to contain the increase in global warming to under 2°C as stipulated in the Paris Agreement [2]. Indeed, through the 'European Green Deal', the EU will invest over one trillion euros to enable the shift from a high- to low-carbon economy [3]. This will promote the adoption of decarbonisation technologies to treat CO_2-rich flue-gases from the carbon-intensive energy, industrial and transportation sectors [1].

Carbon capture and storage (CCS) or utilisation (CCU) technologies can be applied for decarbonising flue-gas. CCU technologies offer the key advantage of recycling CO_2 into products for use in the chemical and food industry, or as building blocks to produce fertilisers, plastics, structural materials, fuels or chemicals whilst displacing the dependency on fossil-fuel resources [4]. Several routes are available for product synthesis from CO_2, involving combinations of physical, chemical, electrochemical, thermo-catalytic or biological processes [5]. The increased availability of low-cost, renewable electric energy makes electrochemical CO_2 reduction the most sustainable route [6]. Electrolysers for CO_2 reduction are approaching commercialisation, but the low product selectivity, high overpotentials, and requirement for expensive and stable catalysts and/or high temperatures remain unresolved challenges [4].

In 2010, Nevin *et al.* reported that the chemolithoautotrophic microorganism *Sporomusa ovata* catalyses CO_2 reduction into acetic acid exploiting reducing power from solid electrodes, with coulombic efficiencies exceeding 85%, in a process called microbial electrosynthesis (MES) [7]. Biological catalysts can achieve higher electricity-to-chemical conversion efficiency (80-99%) and selectivity than metal-based catalysts, reduce materials costs, and allow operation under mild temperature and pressure conditions [8]. Mixed microbial communities from various sources have been shown to form effective, versatile and self-regenerating catalysts into electrodes to convert CO_2 to acetic acid [9,10], or even longer-chain carboxylic acids [11–13] and alcohols [14–16] in MES devices.

When mixed cultures are used as inoculum in MES cells, product diversification occurs as the result of overlapping (bio)electrochemical, acetogenic, solventogenic, and chain elongation pathways [17]. The end-product of MES is related to operating conditions: controlling pH, and abundance of carbon and reducing equivalents can result in a tuneable system, in which selective production of ethanol, butyric or caproic acid, over acetic acid can be achieved [13,18]. However, to date, acetic acid is the main product obtained by CO_2 bioelectroreduction, whereas other organic compounds are typically obtained in mixtures and at low concentration [19]. Thus, strategies to trigger a selective production of valuable, long chain fatty acids and alcohols in MES cells have yet to be developed.

Strategic development of product diversification will be strictly linked to deeper understanding of the microorganisms and mechanisms underpinning the MES process, particularly acetogenesis, solventogenesis and chain elongation, as well as how key species respond to dynamic operating conditions. Planktonic and cathode-attached microbial communities have been analysed to complement chemical and electrochemical data in MES studies [9,20]. However, such studies have provided only overviews on the relatively most abundant species in the community, sometimes only at the conclusion of MES trials during which operating conditions were changed several successive times, and overlook important information on microbial dynamics.

In this study, an MES reactor was operated under different carbon feeding regimens (bicarbonate dosing, and intermittent or continuous CO_2 sparging), achieving stable production of acetic and/or

butyric acid. Distinct from previous studies, the microbial community analysis focused on the differential amplicon sequence variants (ASV) between triplicate samples collected at each operational stage of the MES reactor to unravel the role of microorganisms underpinning hydrogen and carboxylic acid production. The spatial distribution of the cathodic microbial community on the electrode, and co-occurence networks, particularly between microorganisms mediating hydrogen and carboxylic acid production, were also determined. Finally, the cathodic and planktonic communities were compared to assess whether, and to what extent, the composition of the planktonic community is reflected in the cathodic community.

2. Materials and Methods

2.1 Reactor set-up

The h-type microbial electrosynthesis (MES) cells (Section SI 1.1, Fig. S1 in the Supplementary Information, SI) comprised of two acrylic cylinders (8 cm diameter, 12 cm height) connected through a circular (5 cm diameter) proton exchange membrane (Nafion 117, Fuel Cell Store, USA), pre-treated according to Modestra and Mohan [21]. The cathode electrode was an 8×16 cm carbon felt (Panex 30 Fabric PW06, Fuel Cell Store, USA), connected to a Ti wire collector by pressure through a plastic nylon screw, installed on a perforated (48 holes of 6 mm diameter each) acrylic cylinder support. The anode electrode was a 2×2 cm platinised titanium mesh (TI008720, Goodfellow, UK) directly connected to the Ti connector. Connections between electrodes and collectors resulted in a resistance < 5 Ω. An Ag/AgCl reference electrode (BASi RE-5B, Alvatek, UK) was placed inside the cathodic chamber, a few mm distant from the cathode electrode, and kept in position using a rubber ring. The influent line consisted of a CO_2-containing gas bag (10 L) connected to a pump (Verdeflex, The Netherland) and a mass flow meter (FMA-1618A, Omega, UK). A gas bag was connected to the cathodic chamber headspace to maintain atmospheric pressure and facilitate gas analysis. A sampling port was built for collecting liquid samples from both chambers.

2.2 Inoculum, anolyte and catholyte

The inoculum was digested sludge (66.0 ± 3.0 g/L total solids, TS, and 49.8 ± 2.6 g/L volatile solids, VS) from a dairy processing industry (Dairygold, Ireland). The anolyte included (in g/L): KH_2PO_4 (0.33), K_2HPO_4 (0.45), NH_4Cl (1.0), KCl (0.1), NaCl (0.8) and $MgSO_4 \times 7H_2O$ (0.2). Besides this, the catholyte contained 1 mL/L vitamin and 10 mL/L trace metal solution (DSMZ 144). Before inoculation, the catholyte and anolyte had a conductivity of 10.6 and 5.7 mS/cm, respectively. Sodium bicarbonate (3.36 g/L, or 240 mg/L total inorganic carbon, TIC), or CO_2 gas, was added as carbon source according to the stages summarised in Table 1. Bromoethanesulphonic acid (BESA, 0.5 g/L) was added to suppress methanogenic archaea.

2.3 MES reactor operation

The MES cell was started-up with bicarbonate as carbon source, and an applied cathodic potential of -1.0 V *vs.* Ag/AgCl. Temperature was maintained at 25 (± 3)°C and the catholyte was stirred at approximately 400-500 rpm using a stirred hotplate (Cole-Parmer). After one week of operation under abiotic conditions, the cell was inoculated with 1 g_{VS}/L of digested sludge, and BESA (0.5 g/L) was supplied to suppress methanogenic archaea. Five fed-batch cycles of 6-7 days were performed, along with a sixth fed-batch cycle of 14 days, prior to switching the carbon source to gaseous CO_2. At the end of each cycle, 25 mL (5%) catholyte were replaced with fresh medium containing sufficient bicarbonate to re-establish the initial concentration of 240 mg/L TIC. The pH was adjusted to 6.5-7.0 with 3 M HCl at the beginning of each cycle. From day 47, gaseous CO_2, at a flow rate of 2 mL/min, was provided instead of bicarbonate, and 0.5 g/L BESA was again supplied to suppress methanogens. CO_2 was first provided at 4-to-5-day intervals to avoid pH rise (days 47-78), then for two hours thrice weekly (days 79-183), and then continuously (days 183-225) thereafter (with the exception of days 206-219, when no CO_2 was supplied). Catholyte (2 mL) and anolyte (1 mL) samples were collected for chemical analyses thrice and once weekly, respectively, and fresh anolyte and catholyte were supplied to the MES reactor when about 10%

volume (i.e. 50 mL) was removed with samples. BESA was again supplied on day 171 in response to increased methane concentrations in the gas. Gas samples were periodically collected from the gas bag for analysis.

Table 1. Summary of the operation stages

Stage	Days	Carbon source	Regimen	Notes
1	0-47	$NaHCO_3$	Fed-batch	BESA addition on day 0 and 47
2	47-183	CO_2	Fed-batch	BESA addition on day 171
3	183-206	CO_2	Continuous	
4	206-219	None	n.a.	Potentiostat failure on day 209
5	219-225	CO_2	Continuous	

2.4 Microbiological analysis

Catholyte samples for planktonic community analysis (2 mL) were collected in triplicate on days 0, 47, 183, 206 and 225, and stored at -80°C after snap-freezing in liquid nitrogen. Triplicate biofilm samples were collected on day 225 from eight different sections of the cathode for analysis of the attached community, following the procedure described in the Supporting Information (Section SI 1.2). DNA was extracted using a previously described protocol [22]. 16S rRNA genes were amplified using the 515F and 806R primer pair. Initial denaturation (95˚C, 3 min) was followed by 25 cycles of denaturation (95˚C, 30 s), annealing (55˚C, 30 s) and extension (72˚C, 30 s). Library preparation and high-throughput sequencing on the Illumina Miseq platform were performed by FISABIO (Valencia, Spain, *fisabio.san.gva.es*). The Amplicon Sequencing Variants (ASVs) were constructed using Qiime2 workflow. In the final analysis, 5,786 clean ASVs were extracted for n=39 samples on which different multivariate statistical analyses were performed using R software. The details of the bioinformatics steps are provided in the Supporting Information (Section SI 1.3).

2.5 Electrochemical analyses

Electrochemical analyses were performed using a multi-channel potentiostat (VMP3, Biologic, France) in three-electrode set-up. If not otherwise mentioned, all potentials are reported against the Ag/AgCl reference electrode. The MES cell was run in chronoamperometic mode with an applied potential of -1.0 V. Cyclic voltammetries (CV) were performed on days 0, 47, 183 and 225 by switching the potential from 0.0 to -1.0 or -1.2 V at a scan rate of 1 mV/s for four replicate cycles. CV and first derivative analyses were performed using a personalised script on R software, as detailed in the Supplementary Information (Section SI 1.4).

Current densities were normalised to either the cathode projected area (128 cm^2) or the catholyte volume (0.5 L). Cumulative charge was calculated as the integral of the current curve over time. Average coulombic efficiency (CE) was calculated between two consecutive samples based on the ratio of charge converted into carboxylic acids (including acids detected in both the cathodic and anodic chamber).

2.6 MES reactor monitoring

Temperature was measured using a thermocouple thermometer (Digi-Sense Temp 10, Cole-Parmer, UK). Cathodic pH was monitored on-line using a probe (VWR, USA) connected to a controller (Cole Parmer 300, UK), and both cathodic and anodic pH were measured from the samples using a Slimtrode (Hamilton, Switzerland). Anode and cathode conductivity was measured using a conductivity meter (Horiba EC-22, Japan). Total inorganic carbon (TIC) was measured using a TOC analyser (Shimadzu, Japan). Carboxylic acids and alcohols were quantified using a liquid chromatograph (1260 Infinity II, Agilent, USA) with Hi-Plex H column

held at 60°C and refractive index detector (RID). H_2SO_4 (5 mM) was the mobile phase at a 0.7 mL/min flow rate. Gas was analysed using a gas chromatograph (7890B, Agilent, USA) equipped with thermal conductivity detector and Porapak-Q column. Injection port, oven and detector temperatures were 250, 60 and 250°C, respectively.

2.7 SEM analysis

Eight duplicate 1×1 cm samples were collected from the cathode electrode, as detailed in the Supplementary Information (Section SI 1.2), and stored in Petri dishes. The samples were fixed for 2 h using 2% (w/v) each of glutaraldehyde and paraformaldehyde in 0.1 M sodium cacodylate buffer (pH 7.2). Samples were dehydrated by passing twice (15 min each) through an ethanol concentration gradient (30, 50, 70, 90, and 100%), and hexamethyldisilazane (HMDS), and air-dried overnight in a fume hood. Specimens were mounted on aluminium stubs with double-sided carbon tabs, and gold-coated using an Emitech K550 sputter coater. Imaging was using an Hitachi S4700 scanning electron microscope at 15 kV acceleration voltage and 50 µA current.

3. Results and Discussion

3.1 Carboxylic acid production from bicarbonate in fed-batch

During the first week, in which the MES cell was operated under abiotic conditions, a negligible current (below 0.1 A/m^2) was detected, and acetic acid production did not occur. After inoculating the cell (day 0), following a 7-day start-up, acetic acid was produced from bicarbonate at an average rate of 0.9 g/m^2/d on days 7-47 (batch cycles II-VI), reaching a concentration of 0.9 g/L in the catholyte (Fig. 1). Simultaneously, the current demand slowly increased (Fig. 2), confirming the biological origin of the produced acetic acid. However, in this stage, the current remained low (below 0.8 A/m^2) due to the incomplete biofilm formation on the cathode electrode, limiting the rate of acetic acid production. The highest production rate of 1.6 g/m^2/d (41 mg/L/d) was obtained in batch cycle IV, with a coulombic efficiency (CE) of 61% (Table 2). A similar acetic acid production rate (29.4 mg/L/d) was obtained from bicarbonate with mixed cultures using a graphite rod and granular graphite electrode [23]. Production rates above 100 mg/L/d have been obtained using more sophisticated electrode materials, such as carbon nanotubes [10,24].

The CE declined from batch cycle V and was 16% in batch cycle VI. Overall, 35% of the carbon added as bicarbonate in the six batch cycles was recovered as acetic acid. Remaining carbon was likely consumed for microbial growth, in particular during batch cycle I, or diffused outside the MES reactor as CO_2. Traces of methane were identified in the MES reactor headspace, suggesting the onset of methanogenesis favoured by the relatively high cathodic pH (7.9) on days 45-47. In MES reactors, the pH on the cathode surface is even higher than in the catholyte, due to the local production of hydroxyl ions [11], which could favour methanogenic archaea. Methanogens adversely affect the CE by converting MES products (*i.e.* carboxylic acids) or reducing equivalents (*i.e.* hydrogen) to methane.

Table 2. Acetic acid production, average current and coulombic efficiency obtained in the MES cell in the six batch cycles with bicarbonate as carbon source. At the beginning of each batch cycle, bicarbonate was added to restore a concentration of 240 mgC/L.

Batch cycle	Days	Bicarbonate supplied (mgC/L)	Acetic acid production (mgC/L)	Average production rate (g/m^2/d)	Average current (A/m^2)	Coulombic efficiency (%)
I	0-7	240.0	9.5	0.13	0.25	7.7
II	7-14	115.2	72.2	1.01	0.41	36.7
III	14-20	134.4	53.4	0.87	0.42	32.2
IV	20-26	175.7	97.6	1.59	0.41	61.0
V	26-33	172.8	87.6	1.22	0.57	32.3

VI	33-47	240.0	53.2	0.36	0.37	15.9

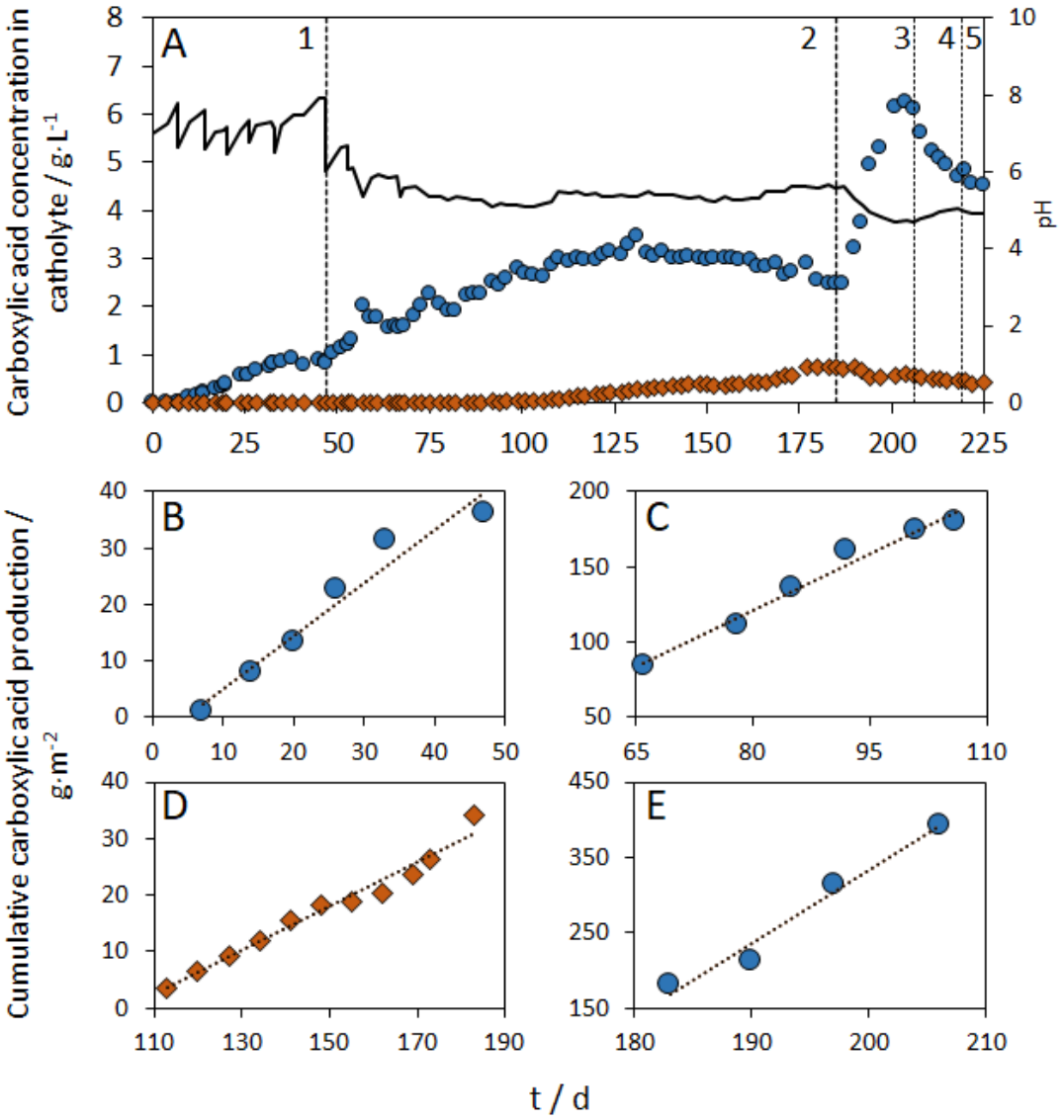

Figure 1. (A) Carboxylic acid concentration (acetic acid, blue circles; butyric acid, orange squares) in the catholyte and pH (black line) over time; numbers 1-5 refer to the operating stages, as summarised in Table 1. **(B-E)** focus on steady-state carboxylic acid production periods with regression curve showing the average production rates in g/m^2/d, taking into account carboxylic acids detected both in the catholyte and anolyte (Fig. S2), and those removed with samples. Rates in g/m^2/d: 0.94 (R^2=0.95); 2.54 (R^2=0.98); 0.39 (R^2=0.97) and 9.68 (R^2=0.97) in B-E, respectively.

3.2 Carboxylic acid production from CO_2 in fed-batch

On day 47, after adding 0.5 mg/L BESA to suppress methanogens and switching the carbon source from bicarbonate to CO_2, the reductive current increased and peaked at 3.5 A/m^2 on day 96 (Fig. 2), indicating development of the electrogenic community on the electrode. On days 96-183, the current slightly decreased due to declining conductivity of both the anolyte and catholyte (Fig. S3), attributed to microbial consumption of electrolytes (e.g. nutrients) present in the catholyte. However, the acetic or butyric acid production rates were not adversely affected (Fig. 1), suggesting the microbial community was not lacking nutrients at any stage. A steady acetic acid

production rate of 2.5 g/m^2/d was achieved on days 66-106, up to 3 g/L acetic acid concentration in the catholyte (Fig. 1). From day 66 onwards, a share of the carboxylic acids migrated from the cathode toward the anode through the membrane, resulting in acetic acid concentrations >2 g/L in the anolyte (Fig. S2). Similar observations were reported from another long-term MES experiment [25], which suggested reactive oxygen species produced at the anode could degrade the membrane. CEs of 21-30% were achieved on days 47-92 (Fig. 2), lower than achieved with bicarbonate due to the low solubility of CO_2 in the pH range 5-6. Solubility can be tackled by maximising the electrode active surface/volume ratio [13], or using gas diffusion electrodes (GDEs) [14,26].

On day 96, the current density plateau coincided with the onset of butyric acid production (Figs. 1 and 2). From day 113, acetic acid production dropped, and its concentration in the catholyte stabilised to about 3 g/L, whereas butyric acid was steadily produced at 0.4 g/m^2/d up to a concentration of 0.7 g/L on day 183 (Fig. 1). On days 171-183, butyric acid was the only carboxylic acid produced with 10-12% CE (Fig. 2). Since acetic acid concentrations were stable on days 113-177, and ethanol was not detected, butyric acid was likely produced from CO_2 through the Wood-Ljungdahl pathway coupled with Acetyl-CoA reduction, rather than *via* non-electrochemical chain elongation [25]. Chain elongation is indeed more favourable at high hydrogen partial pressure [27], whereas this study was conducted at near-atmospheric pressure. Nevertheless, it cannot be excluded that ethanol was produced and immediately consumed for chain elongation. Ethanol production, and subsequent butyric acid production *via* chain elongation, was achieved previously [12] in a tubular MES reactor at hydrogen partial pressures >1 atm, reaching butyric acid production rates of 6.4 g/m^2/d. Similarly, Vassilev *et al.* [13] obtained a mixture of acetic, butyric and caproic acid, and the respective alcohols, from CO_2 through combined acetogenesis, solventogenesis and chain elongation reactions. Conversely, Jourdin *et al.* achieved butyric and caproic acid, but not alcohol, production from CO_2, likely due to the relatively high pH (5.8) preventing solventogenesis [28].

On days 67-183, the pH remained stable at 5.4 (± 0.2) (Fig. 1), due to the balance between H^+ from carboxylic and carbonic acid dissociation, and OH^- production at the cathode [4], which represents a key advantage of MES compared to non-electrochemical carbon recycling technologies. However, despite the low pH, OH^- generation at the cathode can favour methanogens. On day 171, methane was detected at a rate of 20 mL/day, confirming methanogens are only temporarily inhibited by BESA [29], and, thus, BESA was added once again, which slowly decreased methane production (Fig. S4).

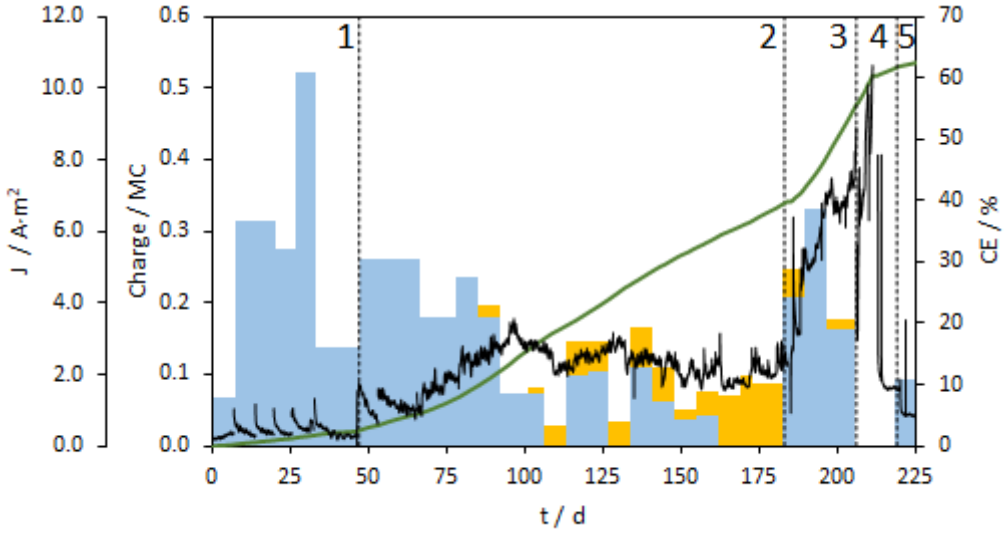

Figure 2. Current (black line) and cumulative charge (green line) generated over time (primary axis) and share of electrons converted into acetic (light blue) and butyric (orange) acid (secondary axis). The coloured areas represent the average coulombic efficiency achieved between two consecutive samples. Numbers 1-5 refer to the operation stages as summarised in Table 1.

3.3 Carboxylic acid production from CO_2 in continuous

From day 183, a constant acetic acid production rate of 9.7 g/m^2/d (0.25 g/L/d) was achieved in response to the continuous CO_2 supply, resulting in a maximum concentration of 6.2 g/L in the catholyte on day 204 (Fig. 1) and CEs up to 40% (Fig. 2). TIC concentration in the catholyte, which was below detection during fed-batch operation, increased to 35 mgC/L on day 187; however, it decreased to <10 mgC/L on day 204, suggesting fast dissolved-carbon fixation by the community (Fig. S5). Both the acetic acid production rate and CE fairly compare with those obtained from gaseous CO_2 with mixed cultures and carbon-based fiber electrodes [19]. More advanced 3-D structured porous electrodes have been shown to increase the acetic acid production rate from CO_2 by two orders of magnitude [19].

The reductive current followed the trend of acetic acid production, increasing from 2 (day 183) to 7 (day 198) A/m^2 prior to stabilising (Fig. 2). Increased current was caused by increased electrons demand for acetic acid production, and by decreased pH from 5.6 (day 185) to 4.7 (day 201) (Fig. 1). Acetic acid production stopped suddenly once the catholyte dropped below its pK_a value of 4.75 (on day 201). At pH 4.71, about 55% of the acetic acid in the catholyte (3.4 g/L) was undissociated, and concentrations >40-50 mM (2.4–3.0 g/L) can be toxic for acetogenic bacteria [30]. The expected current drop, in response to inhibited acetogenesis, did not materialise (Fig. 2). The electron flow was indeed diverted towards hydrogen production with a rate of 185 mL/d on days 197-204 (Fig. S6). It is plausible that (bio)-electrochemically generated hydrogen mediated acetic acid production [31], and acetogenesis inhibition resulted in accumulation of unused hydrogen.

During continuous CO_2 feeding (day 183-206), butyric acid CE remained <5% (Fig. 2) likely due to lower hydrogen partial pressure caused by CO_2 sparging [12], supporting the conclusion that fed-batch operation, alternating low- and high-carbon-availability, triggers butyric acid production. This is in agreement with Arends *et al.* [16], who found that, though continuous operation outperforms batch operation for acetic acid production, low HRTs, and thus high carbon availability, result in lower product diversification. When the CO_2 supply was switched off on days 206-219, however, butyric acid production was not restored, and only acetic acid was produced when continuous CO_2 feeding was provided again on days 219-225 (Fig. 2). This

suggests the acetogenic community was resilient to starvation, and to the brief current interruption due to potentiostat failure on day 209.

3.3 Electrochemical analysis

Cyclic voltammetry analysis (Fig. 3) suggested the development of the cathodic biofilm over time, which was further confirmed by SEM imaging (Fig. S7). Indeed, the potential required for the hydrogen evolution reaction (HER) increased over time, being about -1.0 V and -0.7 V on days 0 and 183, respectively (Fig. 3), indicating increasing catalytic activity in the electrogenic biofilm, supporting previous reports [20,32]. However, the HER over-potential slightly increased on days 183-225, likely due to electroactive community impairment following starvation on days 206-219. Additionally, the more narrow CV curve on day 225 compared to day 183 indicates lower capacitance, and, thus, lower biofilm density on the electrode [33].

First derivative analysis showed the evolution over time of redox-active compounds, potentially mediating electron transfer between the electrode and microorganisms. The reductive peak detected at about -0.5 V on day 0 (Fig. 3), is likely due to traces of electroactive impurities on the electrode surface. On day 47, after six fed-batch cycles with bicarbonate, two further peaks appeared at a potential of -0.205 and -0.868 V, respectively. The peak at -0.205 V suggests the presence of membrane-bound cytochromes used by electroactive microorganisms for electron transfer [21]. The oxidation peak detected at -0.287 V (Fig. S8) on the same day may suggest a reversible (or quasi-reversible) redox system compatible with cytochromes, suggesting that hydrogen evolution at the electrode was catalysed by electrotrophic microorganisms (Section 3.4.1). Interestingly, on day 183 the peak at -0.205 appears to overlap with another reductive peak at -0.297 V. Such a peak, detected when feeding CO_2 but missing when feeding bicarbonate, indicates the presence of further electron shuttles involved in the electron transfer chain for acetic acid or even butyric acid production. Indeed, butyric acid was detected on day 183, but not on day 47. However, further studies are required to confirm this preliminary result.

On day 183, the reductive peak at -0.583 V could be the same peak detected at -0.868 V on day 47, suggesting the presence of electroactive compounds involved in hydrogen production, shifting toward positive potential over time due to the increasing electro-catalytic activity of the biofilm. Tahir *et al.* [34] obtained a similar peak in a CO_2-fed MES reactor, although at a slightly higher potential (-0.557 V), which can be attributed to the better catalytic effect of their MXene-coated cathode than the bare carbon felt used in this study. Neither peak at -0.583 nor -0.297 V, however, was detected on day 225, when much lower acetic acid, and no butyric acid, was detected (Fig. 2).

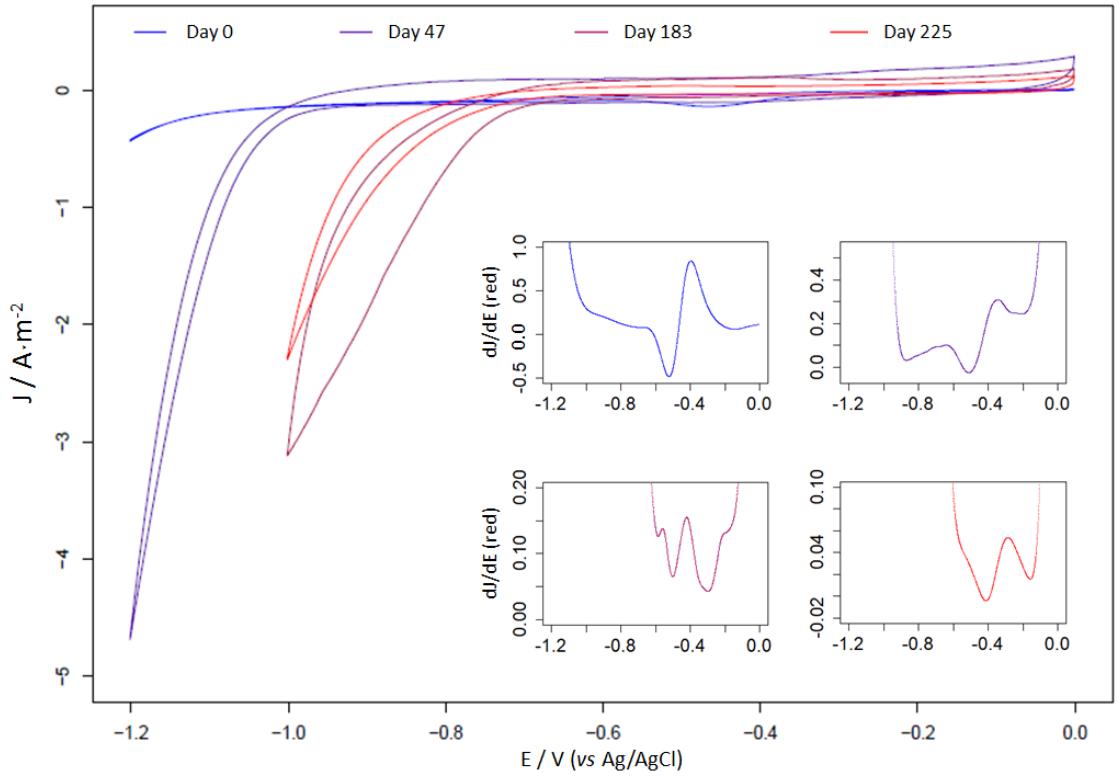

Figure 3. Cyclic voltammetry analysis at different time intervals. The voltage interval was from 0 to -1.2 V when the analysis was performed on days 0 and 47, but the negative end was set to -1.0 on days 183 and 225 due to potentiostat overload. The small squares represent details of the first derivative of the reduction sweeps, oxidation sweeps are available in the Supplementary Information (Fig. S8). CV analysis was done in four replicate cycles, and results reported refer to the third cycle.

3.4 Microbial community analysis

3.4.1 Evolution of the planktonic microbial community

Alpha diversity analysis revealed significantly increased richness and reduced evenness in the planktonic community at day 47 (Fig. 4). However, no significant change in Shannon Entropy occurred. Differential taxa analysis revealed the abundance of several taxa belonging to Bacteroidetes, Synergystetes and Firmicutes increased during days 0-47 (Figs. 4 and S9). Among Bacteroidetes, ASVs belonging to the *Rikenellaceae* family, which was previously associated with hydrogen production in biocathodes [35], significantly increased (Fig. S9). This suggests that *Rikenellaceae* catalysed hydrogen production at the cathode electrode. Since hydrogen was not detected, it is plausible that it was utilised syntrophically by acetogenic *Clostridiales* (Firmicutes) such as *Acetobacterium* and *Acetoanaerobium*, which also increased significantly during the same period (Fig. 4). Representatives from both genera use hydrogen as electron source for acetic acid production from bicarbonate [31,36].

BESA addition on day 0 significantly reduced the abundance of methanogens, such as the acetotrophic *Methanosaeta* (Fig. S9). However, the relative abundance of *Methanobrevibacter*, a hydrogenotrophic methanogen, increased by day 47, (Fig. 4), explaining the traces of methane in the cathode headspace and suggesting BESA does not entirely inhibit the methanogenic community. *Methanobrevibacter* was previously identified in MES reactors, despite BESA addition and low methane production. It was speculated that this genus can obtain energy by catalysing hydrogen production at the cathode [31]. Similarly, Patil *et al.* reported trivial methane

production and suggested that *Methanobacterium* was pushed towards hydrogen production by the excess of reducing equivalents at the cathode [32].

Changing the carbon source from bicarbonate to gaseous CO_2 on day 47 increased the environmental pressure on the microbial community, resulting in significantly reduced alpha diversity (Fig. 4). *Clostridiales* significantly increased during this phase, suggesting their involvement in acetic and butyric acid production (Fig. 2). A significant increase in ASVs assigned to the *Ruminococcaceae* family was observed, in particular *Oscillibacter* sp. and *Caproiciproducens* sp. (Fig. 4), which strongly indicates their role in butyric acid production. Indeed, the *Caproiciproducens galactitolivorans* genome includes genes encoding Butyril-CoA synthesis [37], confirming its capacity for butyric acid production. Although no direct evidence is available on its involvement, *Oscillibacter* sp. were found relatively more abundant concomitantly with middle-chain fatty acid production pathways [38,39].

On days 183-206, continuous CO_2 sparging resulted in further reduced alpha diversity (Fig. 4), indicating the emergence of a highly specialised community. The relative abundance of *Clostridiaceae* further increased, whereas *Ruminococcaceae* significantly declined (Fig. 4). This included ASVs classified in the *Oscillibacter* genus, whereas ASVs belonging to the *Caproiciproducens* genus continued to increase (Fig. 4). Since butyric acid was not produced during this stage, it can be concluded that *Oscillibacter* sp. was the main producer on days 47-183. Besides *Clostridiales* and *Ruminococcaceae*, only *Sulfurospirillum* sp. (*Campylobacterales*) significantly increased from day 183 to day 206 (Fig. S9). *Sulfurospirillum* sp. is a microaerobic organism commonly found among the cathodic communities in MES [20,40], and a role as an oxygen scavenger has been speculated, although it also grows on acetic acid using hydrogen as electron donor [41]. Both are possible in this case, since the acetic acid concentration in the catholyte was as high as 6.2 g/L (Fig. 1), and both hydrogen production at the cathode (Fig. S6) and oxygen production at the anode increased as a response of the current increase (Fig. 2). Some oxygen diffused to the cathodic chamber through the membrane, resulting in concentrations of 2-4% in the headspace. Such oxygen intrusion, together with BESA addition on day 171, resulted in fewer archaea (Fig. S9) and lower methane production (Fig. S4). This suggests low oxygen concentrations may benefit MES, as far as oxygen-scavenging species protect the strictly anaerobic members of the electotrophic community.

Discontinuing the CO_2 supply on days 206-219 lowered the relative abundance of autotrophic *Clostridium* and *Methanobrevibacter* sp. (Figs. 4 and S9). This interrupted acetic acid production (Fig. 1), and acetate was likely consumed by *Methanosaeta* sp. (Fig. S9). The development of the methanogenic community was likely promoted by the current interruption caused by the potentiostat failure on day 209, since it was previously reported that open-circuit operation of MES reactor promotes methanogenesis [42].

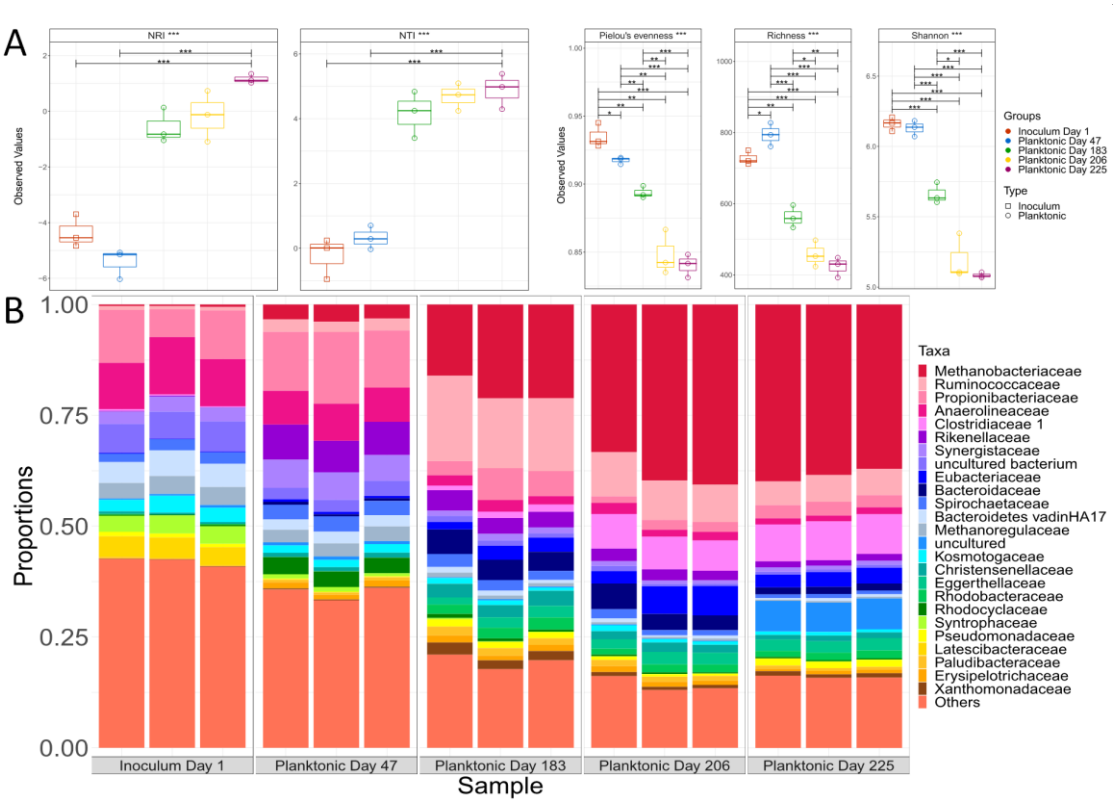

Figure 4. (A) NRI and NTI phylogenetic clustering analysis (See the Supporting Information Section SI 1.3) for details), Pielou's evenness, rarefied richness and Shannon Entropy (Lines of significance depict significant differences as follows: * ($p < 0.05$), ** ($p < 0.01$), or *** ($p < 0.001$) based on ANOVA); **(B)** Taxa plots representing the 25 most abundant microorganisms on the planktonic community over time; **(C)** Heat trees depicting taxa (identified by differential taxa analysis available in Supplementary Table 1), which are up- or down-regulated between samples. The brown colour indicates higher abundance in the latter sample. Cut outs of the *Clostridiales* are presented for ease of use. Whole trees are available in the Supplementary Information (Fig. S9).

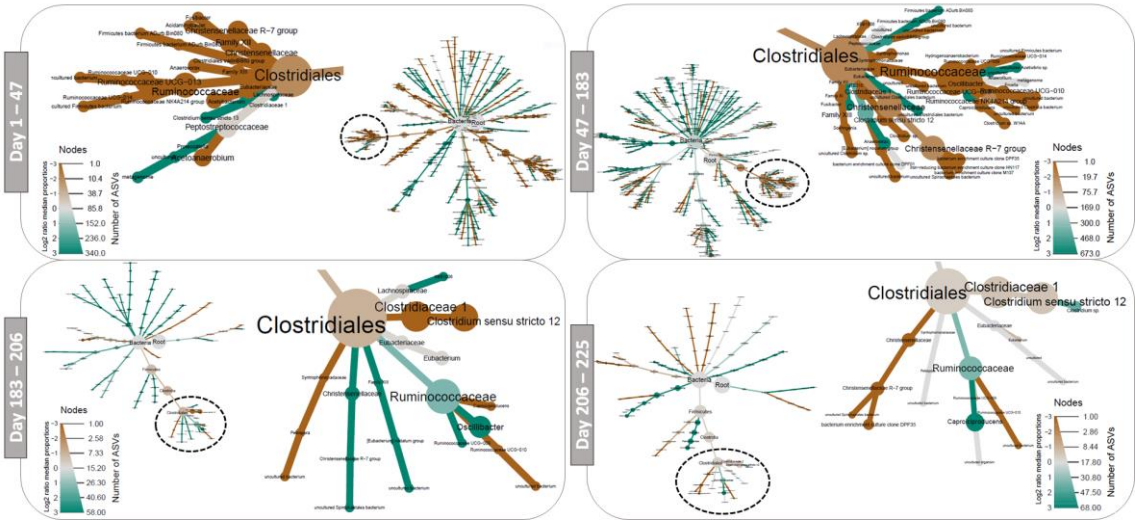

3.4.2 Comparison between the cathodic and planktonic community

After 225 days of operation, the carbon felt surface was covered with a total of 1.83 g of biofilm, with an average of 14.3 (± 3.5) mg/cm^2, against 6.67 g of biomass (13.3 ± 0.8 g/mL) in planktonic

form. Among the top-25 families in the planktonic community, 16 were also abundant in the cathodic community (Figs. 4 and 5), suggesting the planktonic community may provide an estimation of cathodic community composition, which is often difficult to access during MES operation. Nonetheless, PERMANOVA (based on a comparison of all cathode samples to the final planktoic community) revealed significant (R^2 = 0.195, P=0.001) differences in the final planktonic and cathodic communities. Local Contribution to Beta Diversity (LCBD) analysis also revealed significant differences between the final planktonic community and the microbial communities in seven of the eight cathode samples (Fig. 5).

To identify differential taxa between the whole cathode community and the final planktonic community, all cathode samples were grouped and differential taxa analysis was performed. Very few bacterial species were more abundant in the cathodic than in the planktonic community (Fig. S10). Among them, the hydrogenic *Rikenellaceae* and the acetogenic *Eubacteriaceae*, as well as *Sulfurospirillum sp*., were strongly upregulated in the cathode, suggesting their active role in CO_2 reduction to acetic acid. Among acetogens, *Eubacterium* sp., rather than *Acetobacterium* sp., was significantly up-regulated on the cathode. *Eubacterium* sp. was recently shown to perform both acetogenesis *via* the Wood-Ljunghdal pathway and solventogenesis [18], and is therefore a suitable microorganism for MES. Interestingly, *Oscillibacter* sp. was more abundant in the cathodic community, whereas *Caproiciproducens* sp. was more abundant in the planktonic community (Fig. S10), suggesting mediation in differential butyric acid production pathways. Therefore, the capability of *Oscillibacter* sp. for butyric acid production by direct electron transfer requires more investigation.

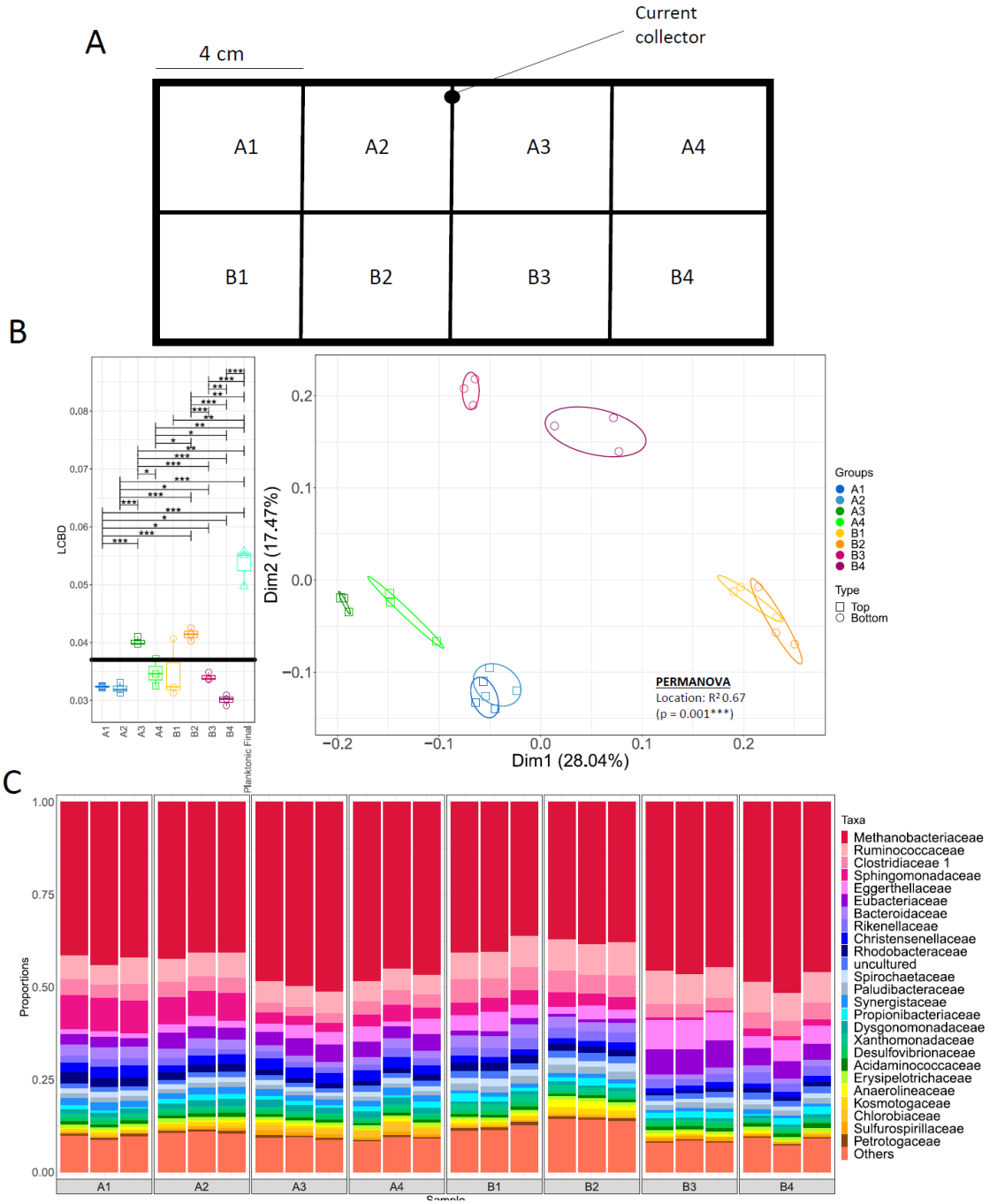

Figure 5. (A) Schematic illustrating the cathode sections sampled; **(B)** Local Contribution to Beta Diversity (including the final planktonic community) and PcoA (cathode samples only) using the Bray-Curtis distance metric. Lines of significance depict significant differences as follows: * ($p < 0.05$), ** ($p < 0.01$), or *** ($p < 0.001$) based on ANOVA. When all cathode samples were grouped together and compared to the final planktonic community PERMANOVA revealed the cathode and planktonic communities to be significantly (P=0.001***) different; **(C)** Top 25 most relatively abundant taxa in the cathode samples.

3.4.3 Spatial variation in the Cathodic Community

Significant differences were observed in alpha diversity of cathode samples, and beta diversity analysis revealed highly significant ($p = 0.001$) localised clustering (Fig. 5). Clustering revealed separation between the top and bottom of the cathode. Only one study previously evaluated the

spatial distribution of the cathodic community in MES, reporting no statistically significant differences between the top, middle and bottom of a carbon cloth electrode [43]. However, the analysis was performed on a methane-producing MES reactor, with a community overwhelmingly dominated by *Archaea* (97% relative abundance). Furthermore, the analysis was performed on the core taxa (OTUs present in all samples at >0.1% relative abundance), whereas, in this study, an ASV-based analysis (which gives variants even down to one nucleotide difference) was implemented, which indicated that communities are more heterogeneous.

SPLS-DA analysis revealed 105 discriminant ASVs among the different cathode locations (Fig. S11). Several microorganisms appear associated with the top of the cathode, including *Methanobrevibacter, Oscillibacter, Eubacterium, Desulfovibrio and Sulfurospirillum* among others. Both *Desulfovibrio* sp. and *Sulfurospirillum* sp. have been reported as members of the core microbiome for CO_2 reduction to acetic acid, together with *Acetobacterium* sp. [44] Furthermore, *Desulfovibrio* sp. was hypothesised to accept electrons from the cathode using cytochromes, formate dehydrogenase and hydrogenases [44], and has been shown to produce hydrogen in MES systems [45], which could explain its higher abundance on the top of the electrode, in proximity to the current collector. Interestingly, *Sulfurospirillum* abundance negatively correlated with distance from the current collector, suggesting non-homogeneous hydrogen production on the cathode surface, with higher production in proximity of the collector.

Genus-level co-occurrence analysis on cathode samples revealed several sub-communities (Fig. S12). Two genera, *Acetobacterium* and *Methanobrevibacter* (brown-shaded sub-community in Figure S12), displayed most connections with other genera, indicating their potential function in shaping the cathode community. More specifically, *Acetobacterium* correlates positively with *Sulfurospurillum,* (further highlighting their potential syntrophy) and negatively with *Clostridium* sp., among others, suggesting competition between the two microorganisms. *Acetobacterium* was abundant in the cathodic community of acetic acid producing MES reactors [10,20,46] and hypothesised as the primary carbon fixer in MES communities [44]. *Methanobrevibacter* also correlated positively with *Sulfurospurillum,* and negatively with *Clostridium* sp., as well as *Caproiciproducens, Methanobacterium,* and *Oscillibacter*, among others. Highly abundant *Acetobacterium* and *Methanobrevibacter* spp. were reported in MES under acetogenic conditions [47] indicating this relationship may not be unique to our system. It is possible that *Methanobrevibacter* and *Acetobacterium* influenced the community by regulating localised hydrogen, CO_2 and acetate concentrations at the cathode interface, supporting micro-environments and inducing spatial heterogeneity in the microbial community.

4. Conclusions

This study shows that higher acetic acid production rates can be achieved feeding MES reactors with gaseous rather than soluble CO_2. Continuous CO_2 sparging resulted in the highest acetic acid production rate of 9.68 $g/m^2/d$, whereas intermittent sparging is necessary to trigger butyric acid production. A novel approach to microbial community analysis, based on significant differences between communities at ASV level, provided explicit information on the role of microorganisms underpinning acetic and butyric acid production in the MES cell. Combined with co-occurrence network and CV analysis, this revealed hydrogen-mediated acetogenesis was mainly carried out by *Clostridium, Eubacterium* and *Acetobacterium*, whereas *Oscillibacter* and *Caproiciproducens* were involved in butyric acid production. Planktonic community analysis may provide an estimation of the species dominating the cathodic community, typically difficult to access in MES reactors. Spatial inhomogeneity of the microbial community on the cathode surface was attributed to differential hydrogen, CO_2 and acetic acid concentrations on the electrode interface. This can represent a barrier when scaling-up bioelectrodes, and suggests multiple connections are required, in full-scale electrodes to promote the establishment of an homogeneous biofilm.

Acknowledgements

This publication was supported by the Science Foundation of Ireland (SFI) Research Professorship Programme on *Innovative Energy Technologies for Bioenergy, Biofuels and a Sustainable Irish Bioeconomy* (IETSBIO3, award 15/RP/2763) and the Research Infrastructure grant *Platform for Biofuel Analysis* (Award no. 16/RI/3401). MI gratefully acknowledges Sardinian Regional Government for the financial support of his PhD scholarship (P.O.R. Sardegna F.S.E. - Operational Programme of the Autonomous Region of Sardinia, European Social Fund 2014-2020 - Axis III Education and training, Thematic goal 10, Investment Priority 10ii), specific goal 10.5. UZI is supported by NERC Independent Research Fellowship (NE/L011956/1). GC and SM were supported by a European Research Council Starting Grant (3C-BIOTECH 261330). GC is supported by the SFI Career Development Award programme (award no. 17/CDA/4658). The authors acknowledge the facilities, and scientific and technical assistance, of the Centre for Microscopy & Imaging at the National University of Ireland Galway (www.imaging.nuigalway.ie).

Conflict of interest

The authors declare no competing interests – financial nor otherwise.

Contributions

PD conceptualised and drafted the manuscript; CS and MI realised the script for CV analysis and assisted in its interpretation; FGC assisted PD in the experimental work; SM and UZI performed the bioinformatics work; all authors revised the manuscript draft; GC and PNLL thoroughly revised the final version for submission.

References

[1] European Environment Agency, The European environment - state and outlook 2020: Knowledge for transition to a sustainable Europe, 2019. https://doi.org/10.2800/96749.

[2] United Nations, Paris Agreement, (2015). https://unfccc.int/files/essential_background/convention/application/pdf/english_paris_agreement.pdf.

[3] European Commission, Financing the green transition: The European Green Deal Investment Plan and Just Transition Mechanism, 2020. https://doi.org/https://ec.europa.eu/commission/presscorner/detail/en/ip_20_17.

[4] R.G. Grim, Z. Huang, M.T. Guarnieri, J.R. Ferrell III, L. Tao, J.A. Schaidle, Transforming the carbon economy: challenges and opportunities in the convergence of low-cost electricity and reductive CO_2 utilization, Energy Environ. Sci. 13 (2020) 472–494. https://doi.org/10.1039/c9ee02410g.

[5] F.M. Baena-Moreno, M. Rodríguez-Galán, F. Vega, B. Alonso-Fariñas, L.F. Vilches Arenas, B. Navarrete, Carbon capture and utilization technologies: a literature review and recent advances, Energy Sources, Part A Recover. Util. Environ. Eff. 41 (2019) 1403–1433. https://doi.org/10.1080/15567036.2018.1548518.

[6] O.G. Sánchez, Y.Y. Birdja, M. Bulut, J. Vaes, T. Breugelmans, D. Pant, Recent advances in industrial CO_2 electroreduction, Curr. Opin. Green Sustain. Chem. 16 (2019) 47–56. https://doi.org/10.1016/j.cogsc.2019.01.005.

[7] K.P. Nevin, T.L. Woodard, A.E. Franks, Z.M. Summers, D.R. Lovley, Microbial Electrosynthesis: Feeding Microbes Electricity To Convert Carbon Dioxide and Water to Multicarbon Extracellular Organic Compounds, MBio. 1 (2010) 2. https://doi.org/10.1128/mBio.00103-10.Editor.

[8] S. Bajracharya, S. Srikanth, G. Mohanakrishna, R. Zacharia, D.P. Strik, D. Pant, Biotransformation of carbon dioxide in bioelectrochemical systems: State of the art and future prospects, J. Power Sources. 356 (2017) 256–273. https://doi.org/10.1016/j.jpowsour.2017.04.024.

[9] R. Mateos, A. Sotres, R.M. Alonso, A. Morán, A. Escapa, Enhanced CO_2 conversion to

acetate through microbial electrosynthesis (MES) by continuous headspace gas recirculation, Energies. 12 (2019) 3297.
[10] L. Jourdin, T. Grieger, J. Monetti, V. Flexer, S. Freguia, Y. Lu, J. Chen, M. Romano, G.G. Wallace, J. Keller, High acetic acid production rate obtained by microbial electrosynthesis from carbon dioxide, Environ. Sci. Technol. 49 (2015) 13566–13574. https://doi.org/10.1021/acs.est.5b03821.
[11] I. Vassilev, F. Kracke, S. Freguia, J. Keller, J.O. Krömer, P. Ledezma, B. Virdis, Microbial electrosynthesis system with dual biocathode arrangement for simultaneous acetogenesis , solventogenesis and carbon chain elongation, Chem. Commun. 55 (2019) 4351–4354. https://doi.org/10.1039/c9cc00208a.
[12] P. Batlle-Vilanova, R. Ganigué, S. Ramió-Pujol, L. Bañeras, G. Jiménez, M. Hidalgo, M.D. Balaguer, J. Colprim, S. Puig, Microbial electrosynthesis of butyrate from carbon dioxide: Production and extraction, Bioelectrochemistry. 117 (2017) 57–64. https://doi.org/10.1016/j.bioelechem.2017.06.004.
[13] I. Vassilev, P.A. Hernandez, P. Batlle-Vilanova, S. Freguia, J.O. Krömer, J. Keller, P. Ledezma, B. Virdis, Microbial electrosynthesis of isobutyric, butyric, caproic acids, and corresponding alcohols from carbon dioxide, ACS Sustain. Chem. Eng. 6 (2018) 8485–8493. https://doi.org/10.1021/acssuschemeng.8b00739.
[14] S. Srikanth, D. Singh, K. Vanbroekhoven, D. Pant, M. Kumar, S.K. Puri, S.S.V. Ramakumar, Electro-biocatalytic conversion of carbon dioxide to alcohols using gas diffusion electrode, Bioresour. Technol. 265 (2018) 45–51. https://doi.org/10.1016/j.biortech.2018.02.058.
[15] J. Gavilanes, C.N. Reddy, B. Min, Microbial electrosynthesis of bioalcohols through reduction of high concentrations of volatile fatty acids, Energy & Fuels. 33 (2019) 4264–4271. https://doi.org/10.1021/acs.energyfuels.8b04215.
[16] J.B.A. Arends, S.A. Patil, H. Roume, K. Rabaey, Continuous long-term electricity-driven bioproduction of carboxylates and isopropanol from CO_2 with a mixed microbial community, J. CO_2 Util. 20 (2017) 141–149. https://doi.org/10.1016/j.jcou.2017.04.014.
[17] M.C.A.A. Van Eerten-Jansen, A. Ter Heijne, T.I.M. Grootscholten, K.J.J. Steinbusch, T.H.J.A. Sleutels, H.V.M. Hamelers, C.J.N. Buisman, Bioelectrochemical production of caproate and caprylate from acetate by mixed cultures, ACS Sustain. Chem. Eng. 1 (2013) 513–518. https://doi.org/10.1021/sc300168z.
[18] R. Blasco-Gómez, S. Ramió-Pujol, L. Bañeras, J. Colprim, M.D. Balaguera, S. Puig, Unravelling the factors that influence the bio-electrorecycling of carbon dioxide towards biofuels, Green Chem. 21 (2019) 684–691. https://doi.org/10.1039/C8GC03417F.
[19] Y. Jiang, H.D. May, L. Lu, P. Liang, X. Huang, Z.J. Ren, Carbon dioxide and organic waste valorization by microbial electrosynthesis and electro-fermentation, Water Res. 149 (2019) 42–55. https://doi.org/10.1016/j.watres.2018.10.092.
[20] E. V Labelle, C.W. Marshall, J.A. Gilbert, H.D. May, Influence of Acidic pH on Hydrogen and Acetate Production by an Electrosynthetic Microbiome, PLoS One. 9 (2014) e109935. https://doi.org/10.1371/journal.pone.0109935.
[21] J.A. Modestra, S.V. Mohan, Microbial electrosynthesis of carboxylic acids through CO_2 reduction with selectively enriched biocatalyst: Microbial dynamics, J. CO_2 Util. 20 (2017) 190–199. https://doi.org/10.1016/j.jcou.2017.05.011.
[22] P. Dessì, P. Chatterjee, S. Mills, M. Kokko, A.-M. Lakaniemi, G. Collins, P.N.L. Lens, Power production and microbial community composition in thermophilic acetate-fed up-flow and flow-through microbial fuel cells, Bioresour. Technol. 294 (2019) 122115. https://doi.org/10.1016/j.biortech.2019.122115.
[23] P. Batlle-Vilanova, S. Puig, R. Gonzalez-Olmos, M.D. Balaguer, J. Colprim, Continuous acetate production through microbial electrosynthesis from CO_2 with microbial mixed culture, J. Chem. Technol. Biotechnol. 91 (2016) 921–927. https://doi.org/10.1002/jctb.4657.
[24] L. Jourdin, S. Freguia, V. Flexer, J. Keller, Bringing High-Rate, CO2-Based Microbial

Electrosynthesis Closer to Practical Implementation through Improved Electrode Design and Operating Conditions, Environ. Sci. Technol. (2016). https://doi.org/10.1021/acs.est.5b04431.
[25] S.M.T. Raes, L. Jourdin, C.J.N. Buisman, D.P.B.T.B. Strik, Continuous Long-Term Bioelectrochemical Chain Elongation to Butyrate, ChemElectroChem. 4 (2017) 386–395. https://doi.org/10.1002/celc.201600587.
[26] S. Bajracharya, K. Vanbroekhoven, C.J.N. Buisman, D. Pant, D.P.B.T.B. Strik, Application of gas diffusion biocathode in microbial electrosynthesis from carbon dioxide, Environ. Sci. Pollut. Res. 23 (2016) 22292–22308. https://doi.org/10.1007/s11356-016-7196-x.
[27] W. de Araújo Cavalcante, R.C. Leitão, T.A. Gehring, L.T. Angenent, S.T. Santaella, Anaerobic fermentation for n-caproic acid production: A review, Process Biochem. 54 (2017) 106–119. https://doi.org/10.1016/j.procbio.2016.12.024.
[28] L. Jourdin, S.M.T. Raes, C.J.N. Buisman, D.P.B.T.B. Strik, Critical biofilm growth throughout unmodified carbon felts allows continuous bioelectrochemical chain elongation from CO_2 up to caproate at high current density, Front. Energy Res. 6 (2018) 7. https://doi.org/10.3389/fenrg.2018.00007.
[29] N. Cabirol, J. Perrier, F. Jacob, B. Fouiliet, P. Chambon, Role of methanogenic and sulfate-reducing bacteria in the reductive dechlorination of tetrachloroethylene in mixed culture, Bull. Environ. Contam. Toxicol. 56 (1996) 817–824. https://doi.org/10.1007/s001289900119.
[30] G. Wang, D.I.C. Wang, Elucidation of growth inhibition and acetic acid production by Clostridium thermoaceticum, Appl. Environ. Microbiol. 47 (1984) 294–298. https://doi.org/10.1128/aem.47.2.294-298.1984.
[31] L. Jourdin, Y. Lu, V. Flexer, J. Keller, S. Freguia, Biologically Induced Hydrogen Production Drives High Rate/High Efficiency Microbial Electrosynthesis of Acetate from Carbon Dioxide, ChemElectroChem. 3 (2016) 581–591. https://doi.org/10.1002/celc.201500530.
[32] S.A. Patil, J.B.A. Arends, I. Vanwonterghem, J. Van Meerbergen, K. Guo, G.W. Tyson, K. Rabaey, Selective enrichment establishes a stable performing community for microbial electrosynthesis of acetate from CO_2, Environ. Sci. Technol. 49 (2015) 8833–8843. https://doi.org/10.1021/es506149d.
[33] F. Harnisch, S. Freguia, A Basic Tutorial on Cyclic Voltammetry for the Investigation of Electroactive Microbial Biofilms, Chem. an Asian J. 7 (2012) 466–475. https://doi.org/10.1002/ASIA.201100740.
[34] K. Tahir, W. Miran, J. Jang, A. Shahzad, M. Moztahida, B. Kim, D.S. Lee, A novel MXene-coated biocathode for enhanced microbial electrosynthesis performance, Chem. Eng. J. 381 (2020) 122687. https://doi.org/10.1016/j.cej.2019.122687.
[35] E. Croese, M.A. Pereira, G.J.W. Euverink, A.J.M. Stams, J.S. Geelhoed, Analysis of the microbial community of the biocathode of a hydrogen-producing microbial electrolysis cell, Appl. Microbiol. Biotechnol. 92 (2011) 1083–1093. https://doi.org/10.1007/s00253-011-3583-x.
[36] K.P. Nevin, S.A. Hensley, A.E. Franks, Z.M. Summers, J. Ou, T.L. Woodard, O.L. Snoeyenbos-West, D.R. Lovley, Electrosynthesis of organic compounds from carbon dioxide is catalyzed by a diversity of acetogenic microorganisms, Appl. Environ. Microbiol. 77 (2011) 2882–2886. https://doi.org/10.1128/AEM.02642-10.
[37] F.R. Bengelsdorf, A. Poehlein, R. Daniel, P. Dürre, Genome sequence of the caproic acid-producing bacterium *Caproiciproducens galactitolivorans* BS-1^T (JCM 30532), Microbiol. Resour. Announc. 8 (2019) e00346-19.
[38] S.L. Wu, J. Sun, X. Chen, W. Wei, L. Song, X. Dai, B.J. Ni, Unveiling the mechanisms of medium-chain fatty acid production from waste activated sludge alkaline fermentation liquor through physiological, thermodynamic and metagenomic investigations, Water Res. 169 (2020) 115218. https://doi.org/10.1016/j.watres.2019.115218.

[39] Q. Wu, W. Guo, X. Bao, X. Meng, R. Yin, J. Du, H. Zheng, X. Feng, H. Luo, N. Ren, Upgrading liquor-making wastewater into medium chain fatty acid: Insights into co-electron donors, key microflora, and energy harvest, Water Res. 145 (2018) 650–659. https://doi.org/10.1016/j.watres.2018.08.046.

[40] S. Tian, H. Wang, Z. Dong, Y. Yang, H. Yuan, Q. Huang, T.-S. Song, J. Xie, Mo_2C-induced hydrogen production enhances microbial electrosynthesis of acetate from CO_2 reduction, Biotechnol. Biofuels. 12 (2019) 71. https://doi.org/10.1186/s13068-019-1413-z.

[41] D.E. Ross, C.W. Marshall, H.D. May, R.S. Norman, Comparative genomic analysis of *Sulfurospirillum cavolei* MES reconstructed from the metagenome of an electrosynthetic microbiome, PLoS One. 11 (2016) e0151214. https://doi.org/10.1371/journal.pone.0151214.

[42] R. Mateos, A. Escapa, M.I. San-Martín, H. De Wever, A. Sotres, D. Pant, Long-term open circuit microbial electrosynthesis system promotes methanogenesis, J. Energy Chem. 41 (2020) 3–6. https://doi.org/10.1016/j.jechem.2019.04.020.

[43] A. Ragab, K.P. Katuri, M. Ali, P.E. Saikaly, Evidence of spatial homogeneity in an electromethanogenic cathodic microbial community, Front. Microbiol. 10 (2019) 1747. https://doi.org/10.3389/fmicb.2019.01747.

[44] C.W. Marshall, D.E. Ross, K.M. Handley, P.B. Weisenhorn, J.N. Edirisinghe, C.S. Henry, J.A. Gilbert, H.D. May, R.S. Norman, Metabolic reconstruction and modeling microbial electrosynthesis, Sci. Rep. 7 (2017) 8391. https://doi.org/10.1038/s41598-017-08877-z.

[45] F. Aulenta, L. Catapano, L. Snip, M. Villano, M. Majone, Linking bacterial metabolism to graphite cathodes: Electrochemical insights into the H_2-producing capability of *Desulfovibrio* sp., ChemSusChem. 5 (2012) 1080–1085. https://doi.org/10.1002/cssc.201100720.

[46] T. Song, H. Zhang, H. Liu, D. Zhang, H. Wang, Y. Yang, H. Yuan, J. Xie, High efficiency microbial electrosynthesis of acetate from carbon dioxide by a self-assembled electroactive biofilm, Bioresour. Technol. 243 (2017) 573–582. https://doi.org/10.1016/j.biortech.2017.06.164.

[47] Y. Xiang, G. Liu, R. Zhang, Y. Lu, H. Luo, High-efficient acetate production from carbon dioxide using a bioanode microbial electrosynthesis system with bipolar membrane, Bioresour. Technol. 233 (2017) 227–235. https://doi.org/10.1016/j.biortech.2017.02.104.